Xiangchun Xuan

Department of Mechanical Engineering,
Clemson University,
Clemson, SC, USA

Received December 28, 2006
Revised March 21, 2007
Accepted March 21, 2007

Short Communication

Revisit of Joule heating in CE: The contribution of surface conductance

We present in this short communication the true form of Joule heating in CE which considers the contribution of surface conductance. This increased conductivity of electrolyte solution within electrical double layer has never been discussed in previous studies. The resultant intensive heat generation near the capillary wall is demonstrated using numerical simulation to produce not a locally strong temperature rise, but an additional temperature elevation in the whole solution compared to the model neglecting surface conductance. The latter effect is, however, negligible in typicall CE while it might become significant in very small channels.

Keywords:
Conductivity / Joule heating / Surface conductance / Temperature
DOI 10.1002/elps.200600854

Joule heating is long known to affect the transport and separation of analytes in CE due to the resultant rise and nonuniformity in the temperature of BGE [1–4]. However, very little attention has been paid to the true form of Joule heating itself. The vast majority of previous studies treated the electrolyte solution as a homogeneous conductor [5–15], and ignored without justification the inhomogeneous Joule heating near the capillary wall. Such nonuniform heat generation arises from the increased conductivity of the solution within the electrical double layer (EDL), *i.e.*, the so-called surface conductance in colloid science [16, 17]. The objective of this communication is to examine the contribution of surface conductance to Joule heating in CE in terms of the temperature variation.

Consider a symmetric electrolyte solution confined in a cylindrical capillary. The ionic redistribution in the solution within EDL causes the variation of liquid conductivity σ [18, 19]

$$\sigma = \sigma_b \cos h\left(\frac{z_v e\psi}{k_B T}\right) \tag{1}$$

where σ_b is the conductivity of the bulk solution, z_v the valence of ions, e the charge of a proton, ψ the EDL potential, k_B the Boltzmann's constant, and T the liquid temperature. Assuming a linear temperature dependence of σ_b

$$\sigma_b = c_b\lambda_0[1 + \alpha(T - T_0)] \tag{2}$$

yields the radial heat conduction equation for the liquid in the absence of thermal end effects [20–22]

$$\frac{1}{r}\frac{d}{dr}\left(r\frac{dT}{dr}\right) = -\frac{c_b\lambda_0 E^2}{k_l}[1 + \alpha(T - T_0)]\ \cos h\left(\frac{z_v e\psi}{k_B T}\right) \tag{3}$$

where c_b is the ionic concentration of the bulk electrolyte solution, λ_0 the molar conductivity of the bulk solution at room temperature T_0, α the temperature coefficient of σ_b, r the radial coordinate, E the externally applied electric field, and k_l the thermal conductivity of the solution. Note that we have assumed a constant k_l in Eq. (3) because the thermal conductivity of aqueous solutions is generally much less sensitive to temperature change in comparison with the electrical conductivity.

The EDL potential ψ appearing in Eq. (3) is determined from the Poisson–Boltzmann equation [16, 17]

$$\frac{1}{r}\frac{d}{dr}\left(r\frac{d\psi}{dr}\right) = \frac{2z_v eN_A c_b}{\varepsilon\varepsilon_0}\sin h\left(\frac{z_v e\psi}{k_B T}\right) \tag{4}$$

where N_A is Avogadro's number, ε_0 the vacuum permittivity, and ε the temperature-dependent dielectric constant of the electrolyte solution. If the effect of EDL potential ψ on electrolyte conductivity is ignored, *i.e.*, zero surface conductance with $\psi = 0$ in Eq. (1), a closed-form solution of the radial temperature profile is readily available from Eq. (3) [23, 24]:

$$T = T_0 + \frac{1}{\alpha}\left[\frac{J_0(q\eta)}{J_0(q) - qJ_1(q)/Bi} - 1\right] \tag{5}$$

Correspondence: Dr. Xiangchun Xuan, Department of Mechanical Engineering, Clemson University, Clemson, SC 29634, USA
E-mail: xcxuan@clemson.edu
Fax: +1-864-656-7299

Abbreviation: EDL, electrical double layer

where $q = \sqrt{c_b \lambda_0 \alpha E^2 R_l^2 / k_l}$ is the Joule heating number (dimensionless) with R_l being the capillary internal radius, J_0 and J_1 the Bessel functions of the first kind, $\eta = r/R_l$ the nondimensional radial coordinate, and $Bi = UR_l/k_l$ the Biot number (dimensionless). In the definition of Bi, U is the overall heat transfer coefficient between the electrolyte solution and the coolant surrounding the capillary outer surface given by $\{R_l[\ln((R_w/R_l)/k_w) + \ln((R_p/R_w)/k_p)) + 1/hR_p]\}^{-1}$, where h is the convective heat transfer coefficient and the subscripts l, w, and p denote the liquid, wall and polyimide coating, respectively. Apparently, the Joule heating number q quantifies the extent of Joule heating in CE, and thus will be used to examine the influence of surface conductance on the liquid temperature profile at different working conditions.

Equations (3) and (4) were solved numerically in a 2-D axial symmetry model* using FEMLAB 3.1 (COMSOL). The obtained temperature profile was then compared with the analytical result in Eq. (5). A nonuniform map mesh (square elements) with much finer grids adjacent to the channel wall was employed to capture the feature within EDL. Specifically, we used ten grid cells in the first 5 Debye lengths (or characteristic EDL length, $1/\kappa = \sqrt{\varepsilon\varepsilon_0 k_B T / 2z_v^2 e^2 N_A c_b}$ [16]) from the capillary wall and five grid cells in the next 15 Debye lengths, which was immediately followed by grid cells on the size of 100 nm until 1 μm away from the capillary wall. Those grid cells beyond 1 μm (to, *e.g.*, 5 μm in a 10 μm capillary) had a uniform size of 1 μm in the radial direction. The size in the axial direction was 1 μm for all grid cells. The imposed boundary conditions include: on the channel wall $r = R_l$, a heat flux $-k_l \partial T/\partial r = U(T - T_0)$ for Eq. (3) and a surface potential $\psi = \zeta$ for Eq. (4); at the channel inlet $z = 0$ and outlet $z = L = 100$ μm, a thermal insulation condition for Eq. (3) and an electrical insulation condition for Eq. (4). The two insulation conditions were applied to render fully developed temperature and EDL potential fields regardless of the capillary length (*i.e.*, the length of the computational domain). The accuracy of the numerical method was benchmarked against Eq. (5) and the analytical solution to Eq. (4) at a small magnitude of zeta potential ζ [16]. The parameters necessary in the simulation are summarized in Table 1 or otherwise noted in the figure captions. The electrolyte solution was assumed to be KCl prepared in pure water. The convective heat transfer coefficient h is 130 $Wm^{-2}K^{-1}$ for free-air cooling while 4000 $Wm^{-2}K^{-1}$ for forced-air cooling [6, 7]. Figure 1 shows the comparison of radial temperature distributions with (symbols) and without (solid lines) consideration of surface conductance in CE cooled by free air (at the applied electric field $E = 5$ kV/cm, $q = 0.125$, left half) and forced air (at $E = 16.50$ kV/cm, $q = 0.413$, right half), respectively. We acknowledge that such high electric fields are rarely used in typical CE, which are presented here for just the demonstration. In both cooling conditions, surface conductance increases Joule heating and thus leads to a higher liquid temperature. However, the temperature profiles still remain parabolic-like despite the fact that the electrolyte conductivity σ within EDL may be much higher than the rest of the solution. Figure 2 demonstrates the variation of σ over the capillary cross-section in the two circumstances considered in Fig. 1. The magnitude of σ near the capillary wall ($\eta = r/R_l = 1$) is over 20 times larger than its bulk value, indicating a 20 times stronger Joule heating within the EDL. Such a highly intensive heat source, however, does not produce a significant local temperature rise because the heat generation can be quickly diffused across the liquid. This explana tion comes from the essentially small Biot number

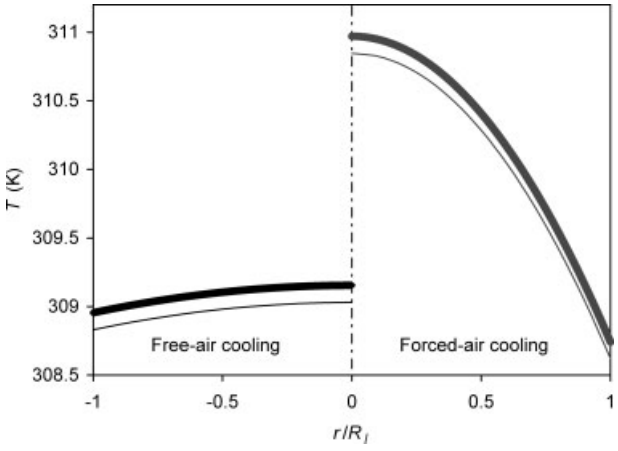

Figure 1. Comparison of radial profiles of liquid temperature T with (symbols) and without (solid lines) consideration of surface conductance in CE at two different cooling conditions: left half, free-air cooling, $E = 5$ kV/cm; right half, forced-air cooling, $E = 16.5$ kV/cm. All other parameters are referred to Table 1.

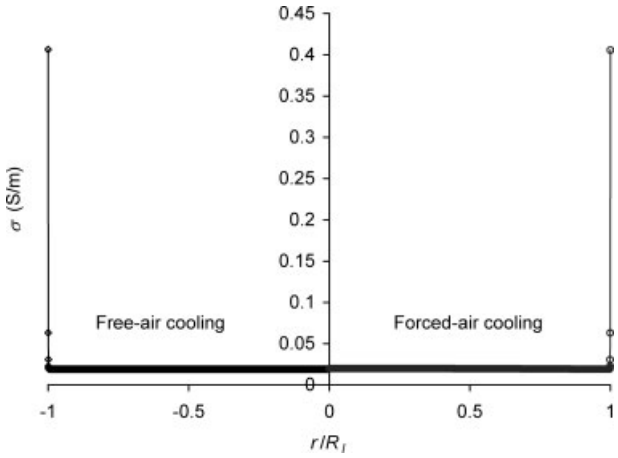

Figure 2. Radial variation of liquid conductivity σ in CE at two different cooling conditions: left half, free-air cooling, $E = 5$ kV/cm; right half, forced-air cooling, $E = 16.5$ kV/cm. All other parameters are referred to Table 1.

* The reason we solved the 1-D Eqs. (3) and (4) in a 2-D axial symmetry model lies in the easier control of both the mesh structure and the mesh density compared to a 1-D axial symmetry model.

Table 1. Summary of parameters used in the calculation unless otherwise noted in the figure captions [25]

Background electrolyte		Capillary	
Property	Value	Property	Value
Concentration c_b	1 mM	Lumen radius R_l	10 μm
Dielectric constant ε	305.7exp(−*T*/219)	Wall radius R_w	160 μm
Thermal conductivity k_l	0.6 $Wm^{-1}K^{-1}$	Polyimide coating radius R_p	180 μm
Molar conductivity λ_0 at T_0	0.015 m^2Smol^{-1}	Wall thermal conductivity k_w	1.5 $Wm^{-1}K^{-1}$
Temperature coefficient α	0.025 K^{-1}	Coating thermal conductivity k_p	0.15 $Wm^{-1}K^{-1}$
Temperature T_0	298 K	Zeta potential ζ	−100 mV

Table 2. Temperature variations with and without (W/O) consideration of surface conductance (SC) in free-air-cooled CE at different conditions

R_l (μm)	c_b (mM)	−ζ (mV)	*E* (kV/cm)	*T* at capillary center (K)		Δ*T* (K)	
				W/O SC	With SC	W/O SC	With SC
10	1	100	6.7	323.31	323.63	0.457	0.460
10	1	50	6.7	323.31	323.38	0.457	0.458
10	10	100	2.13	323.75	323.86	0.465	0.466
25	1	100	2.7	323.37	323.51	0.464	0.465
1	0.1	150	150	308.07	320.25	0.176	0.221

Among these cases, the Joule heating number and the Biot number remained roughly at $q = 0.168$ and $Bi = 0.0367$. The other parameters are referred to Table 1. Note that Δ*T* signifies the temperature difference between the capillary center and the internal wall.

that is about 0.037 in the free-air cooling and 0.41 in the forced-air cooling. One can therefore see a similar temperature profile to that assuming a uniform conductivity.

In addition, we notice in Fig. 1 that the contribution of surface conductance to Joule heating is insignificant. This prediction, which justifies the assumption of a homogeneous liquid conductor in previous studies [5–15], is within our expectation considering the fact that the increase in electrolyte conductivity only takes place within the very thin EDL (the characteristic EDL length $1/\kappa$ is about 10 nm for the case considered in Fig. 1). Referring to Eq. (3), the effect of surface conductance on radial temperature profile is reflected by the distribution of EDL potential ψ. In other words, the parameters that have an influence on ψ will also affect Joule heating in the BGE. Previously, however, ψ is recognized to have an influence on merely the EOF profile [16, 17]. Table 2 compares the temperature variations with and without consideration of surface conductance in free-air cooled CE when one of the three parameters is varied, which are the capillary internal radius R_l, ionic concentration c_b and zeta potential ζ. Among these cases, however, the Joule heating number and the Biot number remain approximately at $q = 0.168$ and $Bi = 0.0367$, so that the temperature profiles can be compared in a fair way. Apparently, the effect of surface conductance on Joule heating decreases when either the electrokinetic radius $\kappa R_l \sim c_b^{0.5} R_l$ expands or the magnitude of zeta potential gets smaller. Such effect, however, remains very little in all the cases under consideration.

We have also presented a special case in Table 2 (see the bottom row), where $R_l = 1$ μm $c_b = 0.1$ mM and $\zeta = -150$ mV. It is once again acknowledged that these parameters, which might be impractical in CE, are used here for just the demonstration of the limiting effect of surface conductance. If the extremely high electric field $E = 150$ kV/cm were assumed available, one could see a 14 K underestimation of the liquid temperature at the capillary center that would be 308.07 K when the surface conductance is neglected. This neglect also causes a 20% underprediction of the temperature difference between the capillary center and wall. Since both the Joule heating number and the Biot number remain roughly the same as the other cases in Table 2, it can be concluded that the effect of surface conductance on the temperature profile has to be taken into consideration in very small capillaries, or more precisely in channels of small electrokinetic radius κR_l.

In summary, we have revisited the Joule heating in CE by considering the contribution of surface conductance. This increased conductivity of electrolyte solution produces more heat generation within EDL, which certainly raises the temperature in the whole solution compared to previous studies assuming a homogeneous conductor. Such an additional

temperature elevation is, however, negligible in typical CE so that the assumption of uniform electrolyte conductivity is justified. We have also demonstrated that the influence of surface conductance on Joule heating might become significant in very small capillaries if an extremely high electric field were applied. As a matter of fact, however, such influence is unlikely to be seen in experiments because other physical effects (*e.g.*, dielectric breakdown of the capillary) would take over before any significant temperature rise in the solution could be observed.

The author would like to thank the generosity of Professor Neumann group in the Department of Mechanical and Industrial Engineering at University of Toronto, so that the numerical simulations involved in this work were able to be performed. Financial support from Clemson University through a start-up package to X. Xuan is also gratefully acknowledged.

References

[1] Hinckley, J. O. N., *J. Chromatogr.* 1975, *109*, 209–217.

[2] Knox, J. H., Grant, I. H., *Chromatographia* 1987, *24*, 135–143.

[3] Gaš, B., Štědrý, M., Kenndler, E., *Electrophoresis* 1997, *18*, 2123–2133.

[4] Rathore, A. S., *J. Chromatogr. A* 2004, *1037*, 431–443.

[5] Rathore, A. S., Reynolds, K. J., Colon, L. A., *Electrophoresis* 2002, *23*, 2918–2928.

[6] Porras, S. P., Marziali, E., Gaš, B., Kenndler, E., *Electrophoresis* 2003, *24*, 1553–1564.

[7] Palonen, S., Jussila, M., Porras, S. P., Riekkola, M., *Electrophoresis* 2004, *25*, 344–354.

[8] Peterson, H. J., Nikolajsen, R. P., Mogensen, K. B., Kutter, J. P., *Electrophoresis* 2004, *25*, 253–269.

[9] Xuan, X. C., Li, D., *Electrophoresis* 2005, *26*, 166–175.

[10] Kang, Y., Yang, C., Huang, X., *Langmuir* 2005, *21*, 7598–7607.

[11] Tang, G., Yan, D., Yang, C., Chai, J. C., Lam, Y. C., *Electrophoresis* 2006, *27*, 628–639.

[12] Chein, R., Yang, Y. C., Lin, Y., *Electrophoresis* 2006, *27*, 640–649.

[13] Huang, K. D., Yang, R. J., *Electrophoresis* 2006, *27*, 1957–1966.

[14] Kates, B., Ren, C. L., *Electrophoresis* 2006, *27*, 1967–1976.

[15] Xuan, X. C., Hu, G., Li, D., *Electrophoresis* 2006, *27*, 3171–3180.

[16] Hunter, R. J., *Zeta Potential in Colloid Science, Principals and Applications*, Academic Press, New York 1981.

[17] Lyklemma, J., *Fundamentals of Interface and Colloid Science, Vol. 1 and 2*, Academic Press, London 1991.

[18] Xuan, X. C., Li, D., *J. Micromech. Microeng.* 2004, *14*, 290–298.

[19] Hildreth, D. J., *Phys. Chem.* 1970, *74*, 2006–2015.

[20] Xuan, X. C., Sinton, D., Li, D., *Int. J. Heat Mass Trans.* 2004, *47*, 3145–3157.

[21] Xuan, X. C., Xu, B., Sinton, D., Li, D., *Lab Chip* 2004, *4*, 230–236.

[22] Xuan, X. C., Li, D., *J. Chromatogr. A* 2005, *1064*, 227–237.

[23] Gobie, W. A., Ivory, C. F., *J. Chromatogr.* 1990, *516*, 191–210.

[24] Xuan, X. C., Li, D., *J. Micromech. Microeng.* 2004, *14*, 1171–1180.

[25] Knox, J. H., *Chromatographia* 1988, *26*, 329–337.

